

# Identification and molecular characterization of mutations in Nucleocapsid Phosphoprotein of SARS-CoV-2

Gajendra Kumar Azad <sup>Corresp. 1</sup>

<sup>1</sup> Department of Zoology, Patna University, Patna, Bihar, India

Corresponding Author: Gajendra Kumar Azad  
Email address: gkazad@patnauniversity.ac.in

SARS-CoV-2 genome encodes four structural protein that include, Spike glycoprotein, Membrane protein, Envelope protein and Nucleocapsid Phosphoprotein (N-protein). The N-protein interacts with viral genomic RNA and helps in packaging. As the SARS-CoV-2 spread to almost all countries worldwide within 2-3 months; it also acquired mutations in its RNA genome. Therefore, this study was conducted with an aim to identify the variations present in N-protein of SARS-CoV-2. Here, we analysed 4163 reported sequence of N-protein from United States of America (USA) and compared with first reported sequence from Wuhan, China. Our study identified 107 mutations that reside all over the N-protein. Further, we show the high rate of mutations in intrinsically disordered regions (IDRs) of N-protein. Our study show 45% residues of IDR2 harbour mutations. The RNA binding domain (RBD) and dimerization domain of N-protein also have mutations at key residues. We further measured the effect of these mutations on N-protein stability and dynamicity and our data reveals that multiple mutations can cause considerable alterations. Altogether, our data strongly suggests that N-protein is one of the mutational hotspot proteins of SARS-CoV-2 that is changing rapidly and these mutations can potentially interferes with various aspects of N-protein functions including its interaction with RNA, oligomerization and signalling events.

1 TITLE

2 Identification and molecular characterization of mutations in Nucleocapsid Phosphoprotein of  
3 SARS-CoV-2

4

5 AUTHORS

6 Gajendra Kumar Azad<sup>1#</sup>

7

8 <sup>1</sup>Department of Zoology, Patna University, Patna-800005, Bihar (India)

9 #Corresponding Author:

10 Gajendra Kumar Azad

11 Email address: [gkazad@patnauniversity.ac.in](mailto:gkazad@patnauniversity.ac.in)

12

13 Keywords: COVID-19; SARS-CoV-2; Mutations; Nucleocapsid Phosphoprotein (N-protein);

14 Infectious diseases; USA

15

16

17

18

19

20

21

22

23

24

25

26

27

28

29

30

31

32

33

34

35

36

37

## 38 ABSTRACT

39 SARS-CoV-2 genome encodes four structural protein that include, Spike glycoprotein,  
40 Membrane protein, Envelope protein and Nucleocapsid Phosphoprotein (N-protein). The N-  
41 protein interacts with viral genomic RNA and helps in packaging. As the SARS-CoV-2 spread to  
42 almost all countries worldwide within 2-3 months; it also acquired mutations in its RNA genome.  
43 Therefore, this study was conducted with an aim to identify the variations present in N-protein of  
44 SARS-CoV-2. Here, we analysed 4163 reported sequence of N-protein from United States of  
45 America (USA) and compared with first reported sequence from Wuhan, China. Our study  
46 identified 107 mutations that reside all over the N-protein. Further, we show the high rate of  
47 mutations in intrinsically disordered regions (IDRs) of N-protein. Our study show 45% residues  
48 of IDR2 harbour mutations. The RNA binding domain (RBD) and dimerization domain of N-  
49 protein also have mutations at key residues. We further measured the effect of these mutations  
50 on N-protein stability and dynamicity and our data reveals that multiple mutations can cause  
51 considerable alterations. Altogether, our data strongly suggests that N-protein is one of the  
52 mutational hotspot proteins of SARS-CoV-2 that is changing rapidly and these mutations can  
53 potentially interferes with various aspects of N-protein functions including its interaction with  
54 RNA, oligomerization and signalling events.

55

## 56 INTRODUCTION

57 In the late December, 2019, Wuhan, the Hubei province of China, reported a surge in  
58 hospitalisation due to pneumonia like symptoms (Zhu et al., 2020). The causative agent was  
59 identified as a severe acute respiratory syndrome coronavirus 2 (SARS-CoV-2) that shares  
60 close similarity with earlier known SARS-CoV (Chen et al., 2020). The SARS-CoV-2 is highly  
61 contagious that lead to its rapid spread worldwide, and in March 2020, the World Health  
62 Organization (WHO) declared the outbreak a pandemic. The disease caused by SARS-CoV-2  
63 has been named as coronavirus disease 19 (COVID-19) that exhibits mild to severe respiratory  
64 distress in the infected individuals. As of 28<sup>th</sup> June, 2020 the COVID-19 has affected all  
65 countries worldwide with close to 10 million reported cases and 0.5 million confirmed deaths.  
66 Further, the epidemiological studies revealed that the mortality rate from COVID-19 is  
67 significantly higher among individuals over 60 years of age with weak immunity (Liu et al.,  
68 2020).

69 The SARS-CoV-2 has positive sense, single stranded RNA genome of approximately 29.8 kb  
70 (Wu et al., 2020b). The majority of viral genome encodes non-structural proteins that are  
71 proteolytically processed from a single Orf1ab polypeptide. SARS-CoV-2 genome also encode  
72 four structural proteins, including the Spike glycoprotein (S), Membrane protein (M), Envelope  
73 protein (E) and Nucleocapsid Phosphoprotein (N) (Wu et al., 2020a). The S, M and E proteins  
74 are located in the lipid bilayer of the virus and contribute to the formation of viral envelope;  
75 however, the N-protein contributes to the viral genomic RNA packaging and remains embedded  
76 in the central core of the virion. N-protein binds with viral genomic RNA and forms helical  
77 structure to maintain the structural integrity of RNA genome (Chang et al., 2014). This is one of  
78 the most abundant structural proteins encoded by the SARS-CoV-2 genome. The SARS-CoV-2  
79 N-protein resembles N-protein from other RNA viruses, known to modulate host intracellular  
80 machinery and also involved in the regulation of virus life cycle (McBride, van Zyl & Fielding,  
81 2014). Evidence show that N-protein is recruited to the Replication-Transcription Complexes  
82 (RTC) via Nsp3 and plays a crucial role in coronaviral life cycle (Cong et al., 2019). The  
83 abrogation of this interaction impairs the stimulation of genomic RNA and viral mRNA  
84 transcription in vivo and in vitro. Furthermore, the N-protein interactions with M promotes  
85 completion of viral assembly by stabilizing N protein-RNA complex, inside the internal virion  
86 (Astuti & Ysrafil, 2020).

87 The crystal structure of N-protein revealed two distinct domains at N and C terminus (Kang et  
88 al., 2020). The domain present towards the N terminus is also known and RNA binding domain  
89 (RBD). The C terminal side harbours dimerization domain which interacts with other N-protein to  
90 make dimer. Apart from these two domains there are three intrinsically disordered regions  
91 (IDRs) at N and C terminal ends as well as between the RBD and dimerization domain of N-  
92 protein. Since, this protein plays critical role in packaging of SARS-CoV-2 RNA genome, the  
93 mutations in N-protein or interfering its function can lead to diverse outcome on viral life cycle  
94 (Rabi Ann Musah, 2005; Chenavas et al., 2013).

95 Moreover, the study of N-protein is also important because of its unique immunological  
96 properties. For instance, earlier study with SARS N-protein has shown that this protein is a  
97 potential candidate for vaccine development because it can induce a strong immunological  
98 response (Liu et al., 2006). A recent study revealed that the B and T cell epitopes of N protein of  
99 SARS-CoV-2 shows close resemblance with that of SARS-CoV indicating that immune targeting  
100 of these identical epitopes may offer protection against this virus (Ahmed, Quadeer & McKay,  
101 2020). Moreover, the sera of COVID-19 patients contains abundant amount of IgA, IgM and IgG  
102 antibodies against N-protein antigen demonstrating the importance of this antigen in host

103 immunity and diagnostics (Shang et al., 2005; Zeng et al., 2020). Therefore, the N-protein is one  
104 of the candidate target molecule that needs to be properly studied to understand its role in virus  
105 pathogenesis, vaccine development and pharmacological implications. Here, we compared the  
106 N-protein sequences obtained from USA with first reported sequence from China to identify the  
107 variations present between them. We have identified 107 mutations and their impact on N-  
108 protein structure and function are discussed.

109

## 110 MATERIALS AND METHODS

### 111 *Sequence retrieval from NCBI-virus-database*

112 The NCBI-virus-database stores the deposited sequences of SARS-CoV-2 which is updated  
113 regularly as the new sequences are reported. As of 23<sup>rd</sup> June 2020, 4163 SARS-CoV-2  
114 sequences of N-protein were deposited from USA. We downloaded these sequences and used  
115 them for analysis in this study. The first reported N-protein sequence from Wuhan was used as  
116 reference sequence or wild type sequence (Wu et al., 2020b). The protein accession  
117 identification number of reference sequence used in this study is YP\_009724397 and rest of the  
118 4163 IDs (reported from USA) are mentioned in supplementary table 1.

119

### 120 *Multiple sequence alignment by Clustal-Omega program*

121 To identify the mutations present in the SARS-CoV-2 N-protein reported from USA, we did  
122 multiple sequence alignments and compared them with the first reported N-protein sequence  
123 (YP\_009724397) from Wuhan, China as described earlier (Azad, 2020). The multiple sequence  
124 alignment was performed using Clustal Omega tool (Madeira et al., 2019).

125

### 126 *Calculation of free energy and vibrational entropy between wild type and mutant N-proteins*

127 In order to measure the impact of mutations identified in this study on the structural dynamicity  
128 and stability of N-protein, we calculated the differences in free energy ( $\Delta\Delta G$ ) and vibrational  
129 entropy ( $\Delta\Delta S_{vib}$ ) ENCoM between wild type and mutants as described earlier (Chand, Banerjee  
130 & Azad, 2020a). This analysis was performed by DynaMut program (Rodrigues, Pires & Ascher,  
131 2018). To perform DynaMut protein modelling we used RCSB protein ID: 6VYO (Kang et al.,  
132 2020) for RBD molecular modelling and RCSB protein ID: 6WJI for dimerization domain  
133 molecular modelling of N-protein. DynaMut also provide the visual representation of fluctuation  
134 in protein structure. The blue colour represents gain in rigidity and red colour represents gain in  
135 flexibility upon mutation.

136

137 *Generation of weblogo to show conservation of N-protein sequences*

138 The weblogo was generated using a webserver as described earlier (Crooks et al., 2004). The  
139 overall height of the stack indicates the sequence conservation at that position, while the height  
140 of symbols within the stack indicates the relative frequency of each amino acid at that position  
141 (Crooks et al., 2004).

142

143 RESULTS

144 *Identification of mutations in IDR1, IDR2 and IDR3 of N-protein*

145 The crystal structure of N-protein of SARS-CoV-2 has been recently solved (Kang et al., 2020),  
146 the structural details show it is comprised of three distinct regions; the N terminal domain  
147 (contains RNA binding domain), C terminal domain (contains dimerization domain) and IDRs as  
148 shown in figure 1. There are three IDRs in N-protein; IDR1 (at the N terminal end), IDR2  
149 (between RBD and CTD) and IDR3 (at the C terminal end). IDR2 is also referred as linker  
150 region (LKR) because it connects RBD and dimerization domain of N-protein. In order to identify  
151 the variations present in N-protein of SARS-CoV-2 reported from the USA, we performed  
152 multiple sequence alignments. Here, we used Clustal Omega program to align 4163 N-protein  
153 polypeptide sequences from USA and compared them with the first reported sequence from  
154 Wuhan, China.

155 Our analysis identified eighteen mutations in IDR1 (Table1). The IDR1 is present from 1-43  
156 residues towards the N terminal end of N-protein. These eighteen mutations correspond to  
157 approximately 40% (18 out of 43) of the residues of IDR1. Among these the most frequently  
158 mutated residues are Gly and Arg (both are mutated at four positions) and Pro residue is  
159 mutated at three different positions in IDR1 (Table 1).

160 Similar analysis with IDR2 identified thirty six mutations which correspond to approximately 45%  
161 of residues of IDR2 (Table 2). The IDR2 is present from 181-256 residues of the N-protein and  
162 connects RBD and dimerization domains. The most frequently mutated residue in IDR2 was  
163 found to be Ser, it is mutated at twelve positions. Further, the Ala, Gly and Arg residues are  
164 mutated at five positions, respectively.

165 Similarly, we identified fifteen mutations in IDR3 (Table 3). The IDR3 is present from 365-419  
166 residues towards the C terminal end of N-protein. Most notable mutations are Thr and Ala  
167 residues are mutated at three positions and Pro, Asp, and Gln are mutated at two positions,  
168 respectively (Table 3). Altogether, we identified sixty nine mutations in intrinsically disordered  
169 regions IDR1, IDR2 and IDR3 of N-protein.

170

171 *Identification of mutations in RBD and dimerization domain of N-protein*

172 The RBD of N-protein starts from 44<sup>th</sup> residue till 180<sup>th</sup> residue. We mapped the mutation in this  
173 region of N-protein and our analysis revealed presence of twenty two mutations (Table 4).  
174 These twenty two mutations also correspond to approximately 16% of the residues of RBD. Our  
175 mutational analysis shows the most frequently mutated residues are Pro and Ala at five  
176 positions and Asp at three positions as shown in table 4.

177 Similar analysis with the dimerization domain of N-protein revealed that it harbours sixteen  
178 mutations (Table 5). The dimerization domain of N-protein starts from 257<sup>th</sup> residue till 364<sup>th</sup>  
179 residue. Our mutational analysis shows Thr is mutated at four positions and Asp at three  
180 positions. Further, only 14 % residues are mutated in this domain which is least among all other  
181 regions of the N-protein identified here. Altogether, we identified thirty eight mutations in RBD  
182 and dimerization domain of N-protein. We have highlighted the location of amino acids in the  
183 representative crystal structure of N-protein that are mutated in RBD (Figure 1B) and  
184 dimerization domain (Figure 1C)

185 Subsequently, we also calculated the frequency of each mutation identified in this study. The  
186 table 6 shows the top ten mutants arranged in descending order of their respective frequencies.  
187 The R203K mutation is having the highest frequency of 4.9% followed by G204R with 4.7%.  
188 Further, we generated weblogo of the 4163 polypeptide sequences of N-protein to observe their  
189 amino acid conservation as shown in figure 1D. Altogether, we have identified 107 mutations in  
190 N-protein that resides in its IDRs and RBD and dimerization domain.

191

192 *Mutations causes alteration in dynamic stability of N-protein*

193 In order to understand the effect of mutations on the stability of the protein we calculated the  
194 differences in free energy ( $\Delta\Delta G$ ) between wild type and mutants. We performed this analysis  
195 using DynaMut program. The positive  $\Delta\Delta G$  corresponds to increase in stability while negative  
196  $\Delta\Delta G$  corresponds to decrease in stability. We performed this analysis with all of the mutations  
197 that reside in RBD and dimerization domain of N-protein. The IDRs do not have proper 3D  
198 structure therefore; this analysis is not accurate for those regions. Our data revealed the  
199 noticeable increase or decrease in free energy in various mutations as shown in table 6. The top  
200 five positive and negative  $\Delta\Delta G$  values are highlighted in table 6. The maximum increase in  $\Delta\Delta G$   
201 was observed for T271I (1.184 kcal/mol) and the highest negative  $\Delta\Delta G$  was obtained for I292T  
202 (-1.952 kcal/mol), both of these mutations reside in dimerization domain of N-protein.

203 We also measured the change in vibrational entropy energy ( $\Delta\Delta S_{\text{vib}}^{\text{ENCoM}}$ ) between the wild  
204 type and the mutants present in RBD and dimerization domain of N-protein (Table 7).Vibration

205 entropy contributes to the configurational-entropy of the proteins (Goethe, Fita & Rubi, 2015).  
206 The negative  $\Delta\Delta S_{\text{vib}}\text{ENCoM}$  of mutant N-protein corresponds to the increase in rigidification and  
207 positive  $\Delta\Delta S_{\text{vib}}\text{ENCoM}$  corresponds to gain in flexibility of the protein structure. The maximum  
208 positive  $\Delta\Delta S_{\text{vib}}\text{ENCoM}$  was obtained for P364L (0.256 kcal.mol<sup>-1</sup>.K<sup>-1</sup>) and negative  
209  $\Delta\Delta S_{\text{vib}}\text{ENCoM}$  was obtained for G284E (-0.844 kcal.mol<sup>-1</sup>.K<sup>-1</sup>). The variation in vibrational  
210 entropy between wild type and mutant can also be visualised as shown in figure 2. The blue  
211 colour corresponds to rigidification in protein structure and red colour corresponds to gain in  
212 flexibility upon mutation. The top three positive and negative  $\Delta\Delta S_{\text{vib}}\text{ENCoM}$  are shown in figure  
213 2 (A-F). Altogether, the data obtained from  $\Delta\Delta G$  and  $\Delta\Delta S_{\text{vib}}\text{ENCoM}$  strongly suggests that the  
214 mutations identified in this study can influence N-protein stability and dynamicity.

215

#### 216 *Intramolecular interactions are altered due to mutations in N-protein*

217 Next, we sought to closely analyse the changes in the intramolecular interactions in some of the  
218 mutants that exhibited significant alterations in  $\Delta\Delta G$ . We compared the intramolecular  
219 interaction for T271I ( $\Delta\Delta G$ : 1.184 kcal/mol) and I292T ( $\Delta\Delta G$ : -1.952 kcal/mol) as these two  
220 mutants showed maximum variations among thirty eight mutants present in RBD and  
221 dimerization domain of N-protein (Table 4 and 5). Our data clearly showed the variations in the  
222 interactions mediated by wild type and mutant residues in the pocket, where these amino acids  
223 resides as shown in figure 3A-B (T271I) , and 3C-D (I292T). Altogether, our data strongly  
224 suggests that the mutants identified in our study are affecting the dynamic stability as well as  
225 intramolecular interactions in the N-protein.

226

#### 227 DISCUSSIONS

228 SARS-CoV-2 is an RNA virus, a causative agent of COVID-19. This virus spread worldwide  
229 within a span of few months and during its spread it also acquired mutations. Several recent  
230 studies reported the appearance of mutations in SARS-CoV-2 proteins (Korber et al., 2020;  
231 Pachetti et al., 2020; Chand, Banerjee & Azad, 2020b). This study was performed with an aim to  
232 identify mutations in N-protein which is one of the main structural proteins of SARS-CoV-2.  
233 Here, we analysed 4163 sequences of N-protein from USA and identified 107 mutations upon  
234 comparison from first reported sequences of the same protein from Wuhan, China. We also  
235 observed around 64% (69 out of 107) of these mutations reside in the IDRs of N-protein. Among  
236 IDRs, the IDR2 harbours 36 mutations that correspond to the most number of mutations  
237 observed in a single distinct region of the N-protein.

238 Earlier studies demonstrated that Ser and Arg-rich linker region (IDR2) plays indispensable role  
239 in intracellular signalling events primarily by phosphorylation at Ser residues (Wootton, Rowland  
240 & Yoo, 2002; McBride, van Zyl & Fielding, 2014). The wild type LKR/ IDR2 contains sixteen Ser  
241 residues, and our study revealed that out of those, twelve serine residues are mutated (table 2).  
242 Therefore, we can safely assume that these mutations of Ser residues might contribute to  
243 alteration of phosphorylation dependent signalling. A recent study shows that S197, S202,  
244 R203 and G204 are important sites of phosphorylation by Aurora kinase A/B, GSK-3 as well as  
245 for its interactions with 14-3-3 protein (Tung & Limtung, 2020). Surprisingly, our study report  
246 mutation in all of these four residues suggesting that these mutant might have altered  
247 phosphorylation signaling. We have also observed that R203 and G204 is the most frequently  
248 mutated residue of N-protein (Table 6). Similar observations were also reported from other  
249 locations (Franco-Munoz et al., 2020). Furthermore, two recent independent studies revealed  
250 that SARS-CoV-2 is capable of suppressing the type-I IFN innate immune pathway possibly due  
251 to the role of N-protein in signalling events (Blanco-Melo et al., 2020; Zhou et al., 2020a) which  
252 can potentially alter the virulence of SARS-CoV-2.

253 We also measured  $\Delta\Delta G$  and  $\Delta\Delta S_{\text{vib}}\text{ENCoM}$  for the mutants that reside in the RBD and  
254 dimerization domain of N-protein. The four mutants that exhibited highest values for  $\Delta\Delta G$  and  
255  $\Delta\Delta S_{\text{vib}}\text{ENCoM}$  identified in our study are T271I, I292T, G284E and P364L. Since, all of them  
256 are in the dimerization domain; therefore, it is possible that these mutations might lead to  
257 alteration in the dimerization potential of N-protein. The structural study of N-protein (C terminal  
258 domain) has revealed that residue 247-279 are essential for RNA binding (Zhou et al., 2020b)  
259 which harbours seven mutations (T247A, K249R, S250F, A252S, S255A, V270L  
260 T271I). The occurrence of these mutations in C terminal domain could possibly affect its  
261 interaction with RNA that might translate into viral RNA packaging and stability. Furthermore,  
262 the N-protein is also proposed as a candidate for vaccine development because it is known to  
263 elicit strong immunological response in SARS-CoV infected patients (Lin et al., 2003). A recent  
264 study shows that several B cell epitope of SARS-CoV were identical with SARS-CoV-2 (Ahmed,  
265 Quadeer & McKay, 2020). This study revealed that one of the most important B and T cell  
266 epitope lies between residues 305-340 of N-protein; however, our study identified multiple  
267 mutations including, P309L, M322I, S327L, T329M, T334I, D340G, D340N in that stretch.  
268 Therefore, it is possible that due to these mutations the properties of epitope might change that  
269 can affect host immunological response. Another mutation, P344S mutation has been  
270 implicated to decrease the protein stability (Khan et al., 2020). Hence, the development of

271 vaccines that target SARS-COV-2 N-protein must consider the mutations that occur in various  
272 populations and locations.

273 Evidences indicate that the N-protein of coronaviruses functions as an RNA chaperones (Zúñiga  
274 et al., 2007, 2010) and also contributes to packaging and maintenance of the RNA genome. It is  
275 also involved in RNA metabolism because N-protein interaction assays have shown the core  
276 stress granule components G3BP1 and G3BP2 are its interacting partners (Gordon et al.,  
277 2020). This interaction can either enhance stress granule induction or inhibit stress granule  
278 formation by sequestering G3BP1/G3BP2 (Hou et al., 2017). Hence, the drugs that can either  
279 inhibit the interactions of RNA with N-protein or interfere with dimerization of N-protein can be a  
280 potential antiviral candidates (Lo et al., 2013). One such drug is Nucleozin and its derivatives  
281 that targets ribonucleoprotein formation in influenza virus by interfering N-protein  
282 oligomerization (Gerritz et al., 2011). Furthermore, a recent study was conducted to identify  
283 inhibitors of SARS-CoV-2 N-protein, identified various promising candidate drugs including  
284 Conivaptan, Ergotamine, Venetoclax and Rifapentine (Onat Kadioglu, 2020). These candidate  
285 drugs interact with the residues that are either mutated (residue 154, 155, 156, 166) or are in  
286 the close vicinity of the mutations (residue 67, 81, 163, 169) identified in our study. Furthermore,  
287 bioinformatics analysis predicted Dihydroergotamine , Rifabutin and Nystatin as a potential  
288 candidate drugs (Onat Kadioglu, 2020) that interacts with a stretch of residues (from residues  
289 150 to 160) of N-protein. Surprisingly, our study revealed that this stretch harbour four mutations  
290 (151, 152, 154 and 156), which can potentially alter the interactions of these drugs with N-  
291 protein. Altogether, the mutation revealed in this study can interfere with various aspects of N-  
292 protein functions that include oligomerization, interaction with RNA and interference in N-protein  
293 mediated signalling events.

294

## 295 CONCLUSIONS

296 In this study we identified 107 mutations in N-protein of SARS-CoV-2 reported from USA.  
297 Further, we demonstrate these mutations can potentially alter dynamic stability of N-protein.  
298 Altogether, the data presented here, warrants further investigations to understand its impact on  
299 SARS-CoV-2 phenotype and drugs that target N-protein.

300

## 301 ACKNOWLEDGEMENTS

302 We would like to acknowledge the Department of Zoology, Patna University, Patna, Bihar (India)  
303 for providing infrastructural support for this study.

304

## 305 FIGURE AND TABLE LEGENDS

306 Figure 1: The schematic structure of Nucleocapsid Phosphoprotein (N-protein) of SARS-CoV-2.  
307 The N-protein comprising of 419 residues is shown. The RNA binding domain, dimerization  
308 domain, intrinsically disordered regions including IRD1, IRD2, and IRD3 are labelled. B-C)  
309 Cartoon representation of crystal structure of the RNA binding domain and dimerization domain  
310 of N-protein. The stick shows the location of residues that are mutated in the respective  
311 domains. The structural representations are made using Autodock software. D) The weblogo  
312 diagram showing the conservation status of polypeptide sequence of N-protein. The overall  
313 height of the stack indicates the sequence conservation at that position, while the height of  
314 symbols within the stack indicates the relative frequency of each amino acid at that position  
315

316 Figure 2: Visual representation of  $\Delta$  Vibrational Entropy Energy between Wild-Type and Mutant  
317 N-protein. The amino acids residues are colored according to the vibrational entropy change as  
318 a consequence of mutation of N-protein. **BLUE** represents a rigidification of the structure and  
319 **RED** a gain in flexibility. (A-C) represents the top three mutants that show rigidification in  
320 structure upon mutation. (D-F) represents the top three mutants that show gain in flexibility upon  
321 mutation. Each panel also shows the mutation and the location of the residues.  
322

323 Figure 3: Visual representation of interatomic interactions contributed by T271I and I292T of N-  
324 protein. Both of these mutants showed maximum positive and negative  $\Delta\Delta G$  among mutants  
325 present in RBD and dimerization domain of N-protein. (A-B) represents threonine to isoleucine  
326 substitution at 271<sup>st</sup> position; (C-D) represents isoleucine to threonine substitution at 292<sup>nd</sup>  
327 position. Wild-type and mutant residues are represented in light-green color. The interactions  
328 made by wild type and mutant residues are highlighted in each panel. The polar interactions are  
329 depicted in red dotted line, hydrophobic interaction in green and weak hydrogen bonds in  
330 orange.

331

332 Table 1: The table show the location and details of mutations identified in IDR1 of N-protein.

333

334 Table 2: The table show the location and details of mutations identified in IDR2.

335

336 Table 3: The table show the location and details of mutations identified in IDR3.

337

338 Table 4: The table show the location and details of mutations identified in RBD of N-protein.

339

340 Table 5: The table show the location and details of mutations identified in dimerization domain  
341 of N-protein.

342

343 Table 6: The frequency of top ten mutations observed in our study

344

345 Table 7: The table show the  $\Delta\Delta G$  and  $\Delta\Delta S_{vib}$  ENCoM of the mutants present in RBD and  
346 dimerization domain of N-protein. DynaMut program was used to calculate both parameters.  
347 The top five positive and negative  $\Delta\Delta G$  values are highlighted in bold digits. The top three  
348 positive and negative  $\Delta\Delta S_{vib}$  ENCoM values are highlighted in bold digits.

349

## 350 REFERENCES

351 Ahmed SF, Quadeer AA, McKay MR. 2020. Preliminary identification of potential vaccine  
352 targets for the COVID-19 Coronavirus (SARS-CoV-2) Based on SARS-CoV Immunological  
353 Studies. *Viruses*. DOI: 10.3390/v12030254.

354 Astuti I, Ysrafil. 2020. Severe Acute Respiratory Syndrome Coronavirus 2 (SARS-CoV-2): An  
355 overview of viral structure and host response. *Diabetes and Metabolic Syndrome: Clinical  
356 Research and Reviews*. DOI: 10.1016/j.dsx.2020.04.020.

357 Azad GK. 2020. Identification of novel mutations in the methyltransferase complex (Nsp10-  
358 Nsp16) of SARS-CoV-2. *Biochemistry and Biophysics Reports*. DOI:  
359 10.1016/j.bbrep.2020.100833.

360 Blanco-Melo D, Nilsson-Payant BE, Liu WC, Uhl S, Hoagland D, Møller R, Jordan TX, Oishi K,  
361 Panis M, Sachs D, Wang TT, Schwartz RE, Lim JK, Albrecht RA, tenOever BR. 2020.  
362 Imbalanced Host Response to SARS-CoV-2 Drives Development of COVID-19. *Cell*. DOI:  
363 10.1016/j.cell.2020.04.026.

364 Chand GB, Banerjee A, Azad GK. 2020a. Identification of twenty-five mutations in surface  
365 glycoprotein (Spike) of SARS-CoV-2 among Indian isolates and their impact on protein  
366 dynamics. *Gene Reports* 21. DOI: 10.1016/j.genrep.2020.100891.

367 Chand GB, Banerjee A, Azad GK. 2020b. Identification of novel mutations in RNA-dependent  
368 RNA polymerases of SARS-CoV-2 and their implications on its protein structure. *PeerJ*  
369 8:e9492. DOI: 10.7717/peerj.9492.

370 Chang CK, Hou MH, Chang CF, Hsiao CD, Huang TH. 2014. The SARS coronavirus  
371 nucleocapsid protein - Forms and functions. *Antiviral Research*. DOI:  
372 10.1016/j.antiviral.2013.12.009.

- 373 Chen N, Zhou M, Dong X, Qu J, Gong F, Han Y, Qiu Y, Wang J, Liu Y, Wei Y, Xia J, Yu T,  
374 Zhang X, Zhang L. 2020. Epidemiological and clinical characteristics of 99 cases of 2019  
375 novel coronavirus pneumonia in Wuhan, China: a descriptive study. *The Lancet*. DOI:  
376 10.1016/S0140-6736(20)30211-7.
- 377 Chenavas S, Crépin T, Delmas B, Ruigrok RWH, Slama-Schwok A. 2013. Influenza virus  
378 nucleoprotein: Structure, RNA binding, oligomerization and antiviral drug target. *Future*  
379 *Microbiology*. DOI: 10.2217/fmb.13.128.
- 380 Cong Y, Ulasli M, Schepers H, Mauthe M, V'kovski P, Kriegenburg F, Thiel V, de Haan CAM,  
381 Reggiori F. 2019. Nucleocapsid Protein Recruitment to Replication-Transcription  
382 Complexes Plays a Crucial Role in Coronaviral Life Cycle. *Journal of Virology*. DOI:  
383 10.1128/jvi.01925-19.
- 384 Crooks GE, Hon G, Chandonia JM, Brenner SE. 2004. WebLogo: A sequence logo generator.  
385 *Genome Research*. DOI: 10.1101/gr.849004.
- 386 Franco-Munoz C, Alvarez-Diaz DA, Laiton-Donato K, Wiesner M, Escandon P, Usme-Ciro JA,  
387 Franco-Sierra ND, Florez-Sanchez AC, Gomez-Rangel S, Calderon LDR, Ramirez JB,  
388 Baez EO, Walteros DM, Martinez MLO, Mercado-Reyes M. 2020. Substitutions in Spike  
389 and Nucleocapsid proteins of SARS-CoV-2 circulating in Colombia. *medRxiv*. DOI:  
390 10.1101/2020.06.02.20120782.
- 391 Gerritz SW, Cianci C, Kim S, Pearce BC, Deminie C, Discotto L, McAuliffe B, Minassian BF, Shi  
392 S, Zhu S, Zhai W, Pendri A, Li G, Poss MA, Edavettal S, McDonnell PA, Lewis HA, Maskos  
393 K, Morfl M, Kiefersauer R, Steinbacher S, Baldwin ET, Metzler W, Bryson J, Healy MD,  
394 Philip T, Zoeckler M, Schartman R, Sinz M, Leyva-Grado VH, Hoffmann HH, Langley DR,  
395 Meanwell NA, Krystal M. 2011. Inhibition of influenza virus replication via small molecules  
396 that induce the formation of higher-order nucleoprotein oligomers. *Proceedings of the*  
397 *National Academy of Sciences of the United States of America*. DOI:  
398 10.1073/pnas.1107906108.
- 399 Gordon DE, Jang GM, Bouhaddou M, Xu J, Obernier K, White KM, O'Meara MJ, Rezelj V V.,  
400 Guo JZ, Swaney DL, Tummino TA, Huettenhain R, Kaake RM, Richards AL, Tutuncuoglu  
401 B, Foussard H, Batra J, Haas K, Modak M, Kim M, Haas P, Polacco BJ, Braberg H, Fabius  
402 JM, Eckhardt M, Soucheray M, Bennett MJ, Cakir M, McGregor MJ, Li Q, Meyer B, Roesch  
403 F, Vallet T, Mac Kain A, Miorin L, Moreno E, Naing ZZC, Zhou Y, Peng S, Shi Y, Zhang Z,  
404 Shen W, Kirby IT, Melnyk JE, Chorba JS, Lou K, Dai SA, Barrio-Hernandez I, Memon D,  
405 Hernandez-Armenta C, Lyu J, Mathy CJP, Perica T, Pilla KB, Ganesan SJ, Saltzberg DJ,  
406 Rakesh R, Liu X, Rosenthal SB, Calviello L, Venkataramanan S, Liboy-Lugo J, Lin Y,

- 407 Huang XP, Liu YF, Wankowicz SA, Bohn M, Safari M, Ugur FS, Koh C, Savar NS, Tran  
408 QD, Shengjuler D, Fletcher SJ, O'Neal MC, Cai Y, Chang JCJ, Broadhurst DJ, Klippsten S,  
409 Sharp PP, Wenzell NA, Kuzuoglu D, Wang HY, Trenker R, Young JM, Cavero DA, Hiatt J,  
410 Roth TL, Rathore U, Subramanian A, Noack J, Hubert M, Stroud RM, Frankel AD,  
411 Rosenberg OS, Verba KA, Agard DA, Ott M, Emerman M, Jura N, von Zastrow M, Verdin  
412 E, Ashworth A, Schwartz O, d'Enfert C, Mukherjee S, Jacobson M, Malik HS, Fujimori DG,  
413 Ideker T, Craik CS, Floor SN, Fraser JS, Gross JD, Sali A, Roth BL, Ruggero D, Taunton J,  
414 Kortemme T, Beltrao P, Vignuzzi M, García-Sastre A, Shokat KM, Shoichet BK, Krogan  
415 NJ. 2020. A SARS-CoV-2 protein interaction map reveals targets for drug repurposing.  
416 *Nature*. DOI: 10.1038/s41586-020-2286-9.
- 417 Hou S, Kumar A, Xu Z, Airo AM, Stryapunina I, Wong CP, Branton W, Tchesnokov E, Götte M,  
418 Power C, Hobman TC. 2017. Zika Virus Hijacks Stress Granule Proteins and Modulates  
419 the Host Stress Response. *Journal of Virology*. DOI: 10.1128/jvi.00474-17.
- 420 Kang S, Yang M, Hong Z, Zhang L, Huang Z, Chen X, He S, Zhou Z, Zhou Z, Chen Q, Yan Y,  
421 Zhang C, Shan H, Chen S. 2020. Crystal structure of SARS-CoV-2 nucleocapsid protein  
422 RNA binding domain reveals potential unique drug targeting sites. *Acta Pharmaceutica  
423 Sinica B*. DOI: 10.1016/j.apsb.2020.04.009.
- 424 Khan MI, Khan ZA, Baig MH, Ahmad I, Farouk A-E, Song YG, Dong J-J. 2020. Comparative  
425 genome analysis of novel coronavirus (SARS-CoV-2) from different geographical locations  
426 and the effect of mutations on major target proteins: An in silico insight. *PloS one*  
427 15:e0238344. DOI: 10.1371/journal.pone.0238344.
- 428 Korber B, Fischer W, Gnanakaran SG, Yoon H, Theiler J, Abfalterer W, Foley B, Giorgi EE,  
429 Bhattacharya T, Parker MD, Partridge DG, Evans CM, Silva T de, LaBranche CC,  
430 Montefiori DC, Group SC-19 G. 2020. Spike mutation pipeline reveals the emergence of a  
431 more transmissible form of SARS-CoV-2. *bioRxiv*. DOI: 10.1101/2020.04.29.069054.
- 432 Lin Y, Shen X, Yang RF, Li YX, Ji YY, He YY, Shi MD, Lu W, Shi TL, Wang J, Wang HX, Jiang  
433 HL, Shen JH, Xie YH, Wang Y, Pei G, Shen BF, Wu JR, Sun B. 2003. Identification of an  
434 epitope of SARS-coronavirus nucleocapsid protein. *Cell research*. DOI:  
435 10.1038/sj.cr.7290158.
- 436 Liu K, Chen Y, Lin R, Han K. 2020. Clinical features of COVID-19 in elderly patients: A  
437 comparison with young and middle-aged patients. *Journal of Infection*. DOI:  
438 10.1016/j.jinf.2020.03.005.
- 439 Liu SJ, Leng CH, Lien SP, Chi HY, Huang CY, Lin CL, Lian WC, Chen CJ, Hsieh SL, Chong P.  
440 2006. Immunological characterizations of the nucleocapsid protein based SARS vaccine

- 441 candidates. *Vaccine*. DOI: 10.1016/j.vaccine.2006.01.058.
- 442 Lo YS, Lin SY, Wang SM, Wang CT, Chiu YL, Huang TH, Hou MH. 2013. Oligomerization of the  
443 carboxyl terminal domain of the human coronavirus 229E nucleocapsid protein. *FEBS*  
444 *Letters*. DOI: 10.1016/j.febslet.2012.11.016.
- 445 Madeira F, Park YM, Lee J, Buso N, Gur T, Madhusoodanan N, Basutkar P, Tivey ARN, Potter  
446 SC, Finn RD, Lopez R. 2019. The EMBL-EBI search and sequence analysis tools APIs in  
447 2019. *Nucleic acids research*. DOI: 10.1093/nar/gkz268.
- 448 McBride R, van Zyl M, Fielding BC. 2014. The coronavirus nucleocapsid is a multifunctional  
449 protein. *Viruses*. DOI: 10.3390/v6082991.
- 450 Onat Kadioglu MSHJGTE. 2020. Identification of novel compounds against three targets of  
451 SARS CoV2 coronavirus by combined virtual screening and supervised machine learning .  
452 *Bull World Health Organ*. DOI: 10.2471/BLT.20.251561.
- 453 Pachetti M, Marini B, Benedetti F, Giudici F, Mauro E, Storici P, Masciovecchio C, Angeletti S,  
454 Ciccozzi M, Gallo RC, Zella D, Ippodrino R. 2020. Emerging SARS-CoV-2 mutation hot  
455 spots include a novel RNA-dependent-RNA polymerase variant. *Journal of Translational*  
456 *Medicine*. DOI: 10.1186/s12967-020-02344-6.
- 457 Rabi Ann Musah. 2005. The HIV-1 Nucleocapsid Zinc Finger Protein as a Target of  
458 Antiretroviral Therapy. *Current Topics in Medicinal Chemistry*. DOI:  
459 10.2174/1568026043387331.
- 460 Rodrigues CHM, Pires DEV, Ascher DB. 2018. DynaMut: Predicting the impact of mutations on  
461 protein conformation, flexibility and stability. *Nucleic Acids Research*. DOI:  
462 10.1093/nar/gky300.
- 463 Shang B, Wang XY, Yuan JW, Vabret A, Wu XD, Yang RF, Tian L, Ji YY, Deubel V, Sun B.  
464 2005. Characterization and application of monoclonal antibodies against N protein of  
465 SARS-coronavirus. *Biochemical and Biophysical Research Communications*. DOI:  
466 10.1016/j.bbrc.2005.08.032.
- 467 Tung HYL, Limtung P. 2020. Mutations in the phosphorylation sites of SARS-CoV-2 encoded  
468 nucleocapsid protein and structure model of sequestration by protein 14-3-3. *Biochemical*  
469 *and Biophysical Research Communications*. DOI: 10.1016/j.bbrc.2020.08.024.
- 470 Wootton SK, Rowland RRR, Yoo D. 2002. Phosphorylation of the Porcine Reproductive and  
471 Respiratory Syndrome Virus Nucleocapsid Protein. *Journal of Virology*. DOI:  
472 10.1128/jvi.76.20.10569-10576.2002.
- 473 Wu A, Peng Y, Huang B, Ding X, Wang X, Niu P, Meng J, Zhu Z, Zhang Z, Wang J, Sheng J,  
474 Quan L, Xia Z, Tan W, Cheng G, Jiang T. 2020a. Genome Composition and Divergence of

475 the Novel Coronavirus (2019-nCoV) Originating in China. *Cell Host and Microbe*. DOI:  
476 10.1016/j.chom.2020.02.001.

477 Wu F, Zhao S, Yu B, Chen YM, Wang W, Song ZG, Hu Y, Tao ZW, Tian JH, Pei YY, Yuan ML,  
478 Zhang YL, Dai FH, Liu Y, Wang QM, Zheng JJ, Xu L, Holmes EC, Zhang YZ. 2020b. A  
479 new coronavirus associated with human respiratory disease in China. *Nature*. DOI:  
480 10.1038/s41586-020-2008-3.

481 Zeng W, Liu G, Ma H, Zhao D, Yang Y, Liu M, Mohammed A, Zhao C, Yang Y, Xie J, Ding C,  
482 Ma X, Weng J, Gao Y, He H, Jin T. 2020. Biochemical characterization of SARS-CoV-2  
483 nucleocapsid protein. *Biochemical and Biophysical Research Communications*. DOI:  
484 10.1016/j.bbrc.2020.04.136.

485 Zhou Z, Ren L, Zhang L, Zhong J, Xiao Y, Jia Z, Guo L, Yang J, Wang C, Jiang S, Yang D,  
486 Zhang G, Li H, Chen F, Xu Y, Chen M, Gao Z, Yang J, Dong J, Liu B, Zhang X, Wang W,  
487 He K, Jin Q, Li M, Wang J. 2020a. Heightened Innate Immune Responses in the  
488 Respiratory Tract of COVID-19 Patients. *Cell Host and Microbe*. DOI:  
489 10.1016/j.chom.2020.04.017.

490 Zhou R, Zeng R, von Brunn A, Lei J. 2020b. Structural characterization of the C-terminal  
491 domain of SARS-CoV-2 nucleocapsid protein. *Molecular Biomedicine* 1:2. DOI:  
492 10.1186/s43556-020-00001-4.

493 Zhu N, Zhang D, Wang W, Li X, Yang B, Song J, Zhao X, Huang B, Shi W, Lu R, Niu P, Zhan F,  
494 Ma X, Wang D, Xu W, Wu G, Gao GF, Tan W. 2020. A novel coronavirus from patients  
495 with pneumonia in China, 2019. *New England Journal of Medicine*. DOI:  
496 10.1056/NEJMoa2001017.

497 Zúñiga S, Cruz JLG, Sola I, Mateos-Gómez PA, Palacio L, Enjuanes L. 2010. Coronavirus  
498 Nucleocapsid Protein Facilitates Template Switching and Is Required for Efficient  
499 Transcription. *Journal of Virology*. DOI: 10.1128/jvi.02011-09.

500 Zúñiga S, Sola I, Moreno JL, Sabella P, Plana-Durán J, Enjuanes L. 2007. Coronavirus  
501 nucleocapsid protein is an RNA chaperone. *Virology*. DOI: 10.1016/j.virol.2006.07.046.  
502

**Table 1** (on next page)

## IDR1 Mutations

The table show the location and details of mutations identified in IDR1 of N-protein.

1 Table 1:

S. No.	Wild type residue	Position of mutation	Mutated residue
1	Asp	3	Tyr
2	Asn	4	Asp
3	Pro	6	Thr
4	Gln	9	His
5	Pro	13	Leu
6	Arg	14	His
7	Gly	18	Cys
8	Gly	19	Arg
9	Pro	20	Leu
10	Asp	22	Tyr
11	Ser	23	Thr
12	Gly	30	Ala
13	Glu	31	Asp
14	Arg	32	Leu
15	Gly	34	Leu
16	Ala	35	Thr
17	Arg	36	Leu
18	Arg	40	Cys
19	Arg	40	Leu

2

**Table 2** (on next page)

IDR2 mutations

The table show the location and details of mutations identified in IDR2.

1 Table 2:

S. No.	Wild type residue	Position of mutation	Mutated residue
1	Ser	183	Tyr
2	Arg	185	Cys
3	Arg	185	Leu
4	Ser	187	Leu
5	Ser	188	Leu
6	Ser	190	Ile
7	Arg	191	Leu
8	Asn	192	Ser
9	Ser	193	Ile
10	Ser	194	Leu
11	Arg	195	Ile
12	Ser	197	Leu
13	Pro	199	Ser
14	Ser	202	Asn
15	Arg	203	Lys
16	Arg	203	Met
17	Gly	204	Arg
18	Thr	205	Ile
19	Ala	208	Gly
20	Arg	209	Lys
21	Arg	209	Thr
22	Ala	211	Ser
23	Gly	212	Cys
24	Asn	213	Tyr
25	Gly	215	Ser
26	Ala	218	Val
27	Ala	220	Thr
28	Gln	229	His
29	Ser	232	Arg
30	Ser	232	Thr
31	Met	234	Ile
32	Ser	235	Pro
33	Ser	235	Phe
34	Gly	236	Val
35	Gly	238	Cys
36	Gly	243	Cys
37	Thr	247	Ala
38	Lys	249	Arg
39	Ser	250	Phe

40	Ala	252	Ser
41	Ser	255	Ala

2

**Table 3** (on next page)

IDR3 mutations

The table show the location and details of mutations identified in IDR3.

1 Table 3:

<b>S. No.</b>	<b>Wild type residue</b>	<b>Position of mutation</b>	<b>Mutated residue</b>
1	Pro	365	Ser
2	Pro	365	Leu
3	Asp	377	Tyr
4	Asp	377	Gly
5	Thr	379	Ile
6	Gln	380	His
7	Ala	381	Val
8	Pro	383	Ser
9	Pro	383	Leu
10	Gln	386	Lys
11	Gln	386	His
12	Thr	391	Ile
13	Thr	393	Ile
14	Ala	397	Ser
15	Ala	398	Val
16	Asp	399	Glu
17	Ser	413	Ile
18	Ser	416	Leu

2

3

4

**Table 4**(on next page)

RBD mutations

The table show the location and details of mutations identified in RBD of N-protein

1 Table 4:

<b>S. No.</b>	<b>Wild type residue</b>	<b>Position of mutation</b>	<b>Mutated residue</b>
1	Pro	46	Ser
2	Glu	62	Val
3	Pro	67	Ser
4	Asp	81	Tyr
5	Ala	90	Ser
6	Ala	119	Ser
7	Pro	122	Leu
8	Ala	125	Thr
9	Asp	128	Tyr
10	Asn	140	Thr
11	Pro	142	Ser
12	Asp	144	Tyr
13	Asp	144	His
14	Ile	146	Phe
15	Pro	151	Leu
16	Ala	152	Ser
17	Asn	154	Tyr
18	Ala	156	Ser
19	Gln	163	Arg
20	Thr	166	Ile
21	Lys	169	Arg
22	Ser	180	Ile

2

**Table 5** (on next page)

Dimerization domain mutations

The table show the location and details of mutations identified in dimerization domain of N-protein.

1 Table 5:

<b>S. No.</b>	<b>Wild type residue</b>	<b>Position of mutation</b>	<b>Mutated residue</b>
1	Val	270	Leu
2	Thr	271	Ile
3	Gly	284	Glu
4	Gln	289	His
5	Ile	292	Thr
6	Gln	294	Leu
7	Asp	297	Val
8	Pro	309	Leu
9	Met	322	Ile
10	Ser	327	Leu
11	Thr	329	Met
12	Thr	334	Ile
13	Asp	340	Gly
14	Asp	340	Asn
15	Asp	348	Tyr
16	Thr	362	Ile
17	Pro	364	Leu

2

**Table 6** (on next page)

Frequency of N-protein mutations

The frequency of top 10 mutations observed in this study

## 1 Table 6:

Mutation	Number of samples that harbour the mutation	% frequency
R203K	207	4.97357
G204R	196	4.709274
E62V	39	0.937049
A208G	24	0.576646
S183Y	20	0.480538
S194L	18	0.432484
T362I	16	0.384431
T205I	15	0.360404
P13L	11	0.264296
R185C	10	0.240269

2

**Table 7** (on next page) $\Delta\Delta G$  and  $\Delta\Delta S_{vib}$  ENCoM calculations

The table show the  $\Delta\Delta G$  and  $\Delta\Delta S_{vib}$  ENCoM of the mutants present in RBD and dimerization domain of N-protein. DynaMut programme was used to calculate both parameters. The top five positive and negative  $\Delta\Delta G$  values are highlighted in bold digits. The top three positive and negative  $\Delta\Delta S_{vib}$  ENCoM values are highlighted in bold digits.

1 Table 7:

S. No.	Mutant	PDB ID	$\Delta\Delta G$ (kcal/mol )	$\Delta\Delta S_{vib}ENCoM$ (kcal.mol <sup>-1</sup> .K <sup>-1</sup> )
1	E62V	6VYO	0.105	0.091
2	P67S	6VYO	<b>-0.486</b>	0.16
3	D81Y	6VYO	0.454	-0.425
4	A90S	6VYO	0.274	0.043
5	A119S	6VYO	0.073	-0.069
6	P122L	6VYO	<b>-0.166</b>	-0.049
7	A125T	6VYO	<b>-0.565</b>	-0.022
8	D128Y	6VYO	<b>0.846</b>	-0.236
9	N140T	6VYO	0.318	-0.177
10	P142S	6VYO	0.26	-0.17
11	D144Y	6VYO	0.291	-0.293
12	D144H	6VYO	-0.036	0.06
13	I146F	6VYO	0.708	<b>-0.837</b>
14	P151L	6VYO	<b>0.771</b>	-0.14
15	A152S	6VYO	0.298	-0.051
16	N154Y	6VYO	-0.096	-0.063
17	A156S	6VYO	0.428	-0.256
18	Q163R	6VYO	-0.092	-0.017
19	T166I	6VYO	0.194	-0.055
20	K169R	6VYO	0.231	0.077
21	V270L	6WJI	0.679	-0.194
22	T271I	6WJI	<b>1.184</b>	-0.472
23	G284E	6WJI	0.553	<b>-0.844</b>
24	Q289H	6WJI	0.18	<b>0.181</b>
25	I292T	6WJI	<b>-1.952</b>	<b>0.186</b>
26	Q294L	6WJI	0.447	-0.078
27	D297V	6WJI	-0.113	-0.072
28	P309L	6WJI	<b>0.887</b>	<b>-0.524</b>
29	M322I	6WJI	<b>-0.348</b>	0.045
30	S327L	6WJI	<b>0.894</b>	-0.259
31	T329M	6WJI	0.569	-0.189
32	T334I	6WJI	0.236	-0.115
33	D340G	6WJI	0.398	-0.114
34	D340N	6WJI	0.194	-0.088
35	D348Y	6WJI	0.136	-0.121
36	T362I	6WJI	0.396	0.047
37	P364L	6WJI	-0.061	<b>0.256</b>

2

# Figure 1

The schematic structure of Nucleocapsid Phosphoprotein (N protein) of SARS-CoV-2.

The schematic structure of Nucleocapsid Phosphoprotein (N-protein) of SARS-CoV-2. The N-protein comprising of 419 residues is shown. The RNA binding domain, dimerization domain, intrinsically disordered regions including IRD1, IRD2, and IRD3 are labelled. B-C) Cartoon representation of crystal structure of the RNA binding domain and dimerization domain of N-protein. The stick shows the location of residues that are mutated in the respective domains. The structural representations are made using Autodock software. D) The weblogo diagram showing the conservation status of polypeptide sequence of N-protein. The overall height of the stack indicates the sequence conservation at that position, while the height of symbols within the stack indicates the relative frequency of each amino acid at that position



## Figure 2

Visual representation of  $\Delta$  Vibrational Entropy Energy between Wild-Type and Mutant N protein.

The amino acids residues are colored according to the vibrational entropy change as a consequence of mutation of N-protein. **BLUE** represents a rigidification of the structure and **RED** a gain in flexibility. (A-C) represents the top three mutants that show rigidification in structure upon mutation. (D-F) represents the top three mutants that show gain in flexibility upon mutation. Each panel also shows the mutation and the location of the residues.

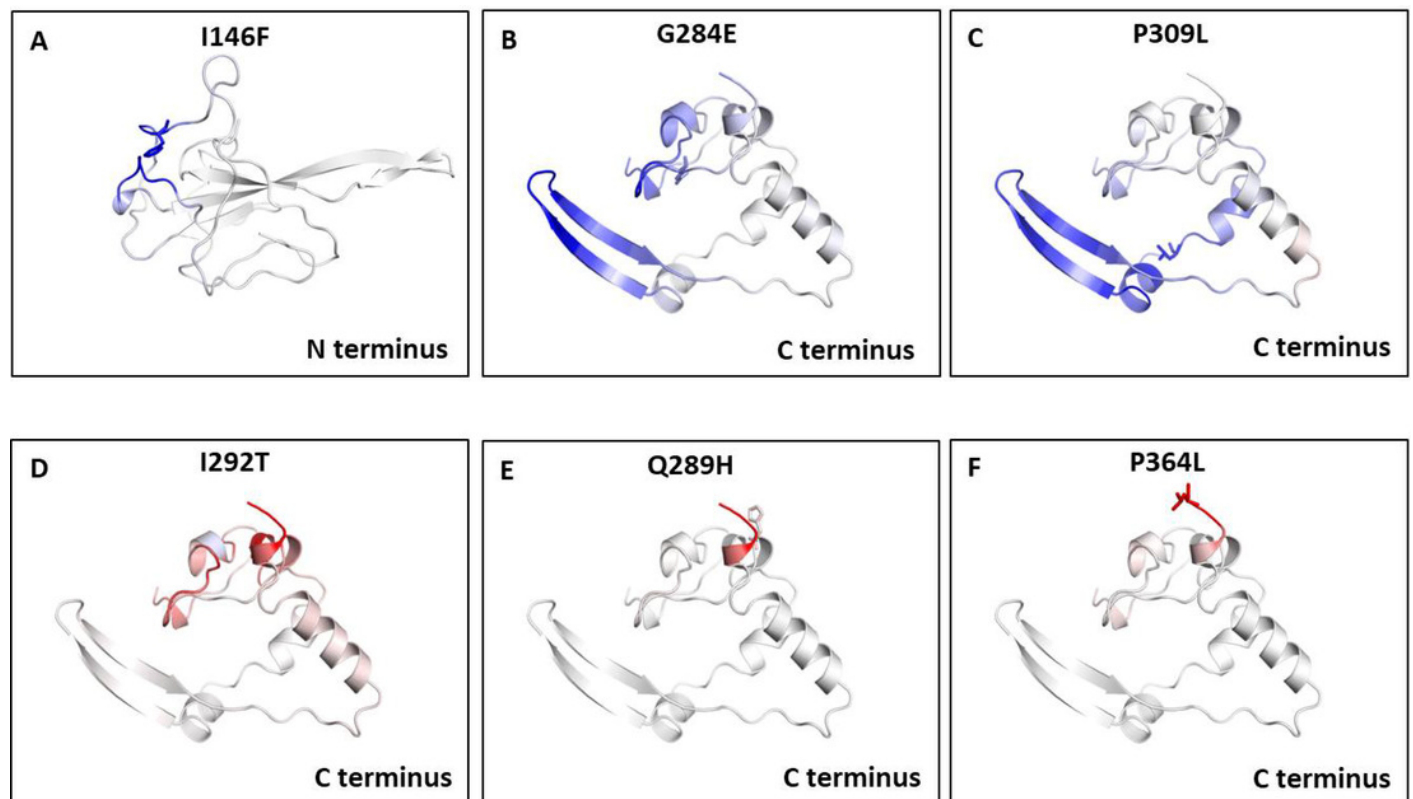


## Figure 3

Analysis of interatomic interactions.

Visual representation of interatomic interactions contributed by T271I and I292T of N-protein. Both of these mutants showed maximum positive and negative  $\Delta\Delta G$  among mutants present in RBD and dimerization domain of N-protein. (A-B) represents threonine to isoleucine substitution at 271<sup>st</sup> position; (C-D) represents isoleucine to threonine substitution at 292<sup>nd</sup> position. Wild-type and mutant residues are represented in light-green color. The interactions made by wild type and mutant residues are highlighted in each panel. The polar interactions are depicted in red dotted line, hydrophobic interaction in green and weak hydrogen bonds in orange.

